Published in final edited form as:

Mol Imaging Biol. 2020 February ; 22(1): 190–197. doi:10.1007/s11307-019-01375-w.

Semiquantitative Parameters in PSMA-Targeted PET Imaging with [^{18}F]DCFPyL: Impact of Tumor Burden on Normal Organ Uptake

Rudolf A. Werner[1,2,3,4], **Ralph A. Bundschuh**[5], **Lena Bundschuh**[5], **Constantin Lapa**[2], **Yafu Yin**[1,6,7], **Mehrbod S. Javadi**[1], **Andreas K. Buck**[2,3], **Takahiro Higuchi**[2,3,8], **Kenneth J. Pienta**[9], **Martin G. Pomper**[1,9], **Martin A. Lodge**[1], **Michael A. Gorin**[1,9], **Steven P. Rowe**[1,9]

[1]The Russell H. Morgan Department of Radiology and Radiological Science, Johns Hopkins University School of Medicine, Baltimore, MD, USA

[2]Department of Nuclear Medicine, University Hospital Wurzburg, Germany

[3]Comprehensive Heart Failure Center, University Hospital Wurzburg, Germany

[4]Department of Nuclear Medicine, Hannover Medical School, Hannover, Germany

[5]Department of Nuclear Medicine, University Medical Center Bonn, Germany

[6]Department of Nuclear Medicine, The First Hospital of China Medical University, Shenyang, China

[7]Department of Nuclear Medicine, Xinhua Hospital, Shanghai Jiao Tong University School of Medicine, Shanghai, China

[8]Okayama University Graduate School of Medicine, Dentistry and Pharmaceutical Sciences, Okayama, Japan

[9]The James Buchanan Brady Urological Institute and Department of Urology, Johns Hopkins University School of Medicine, Baltimore, MD, USA

Abstract

Correspondence: Steven P. Rowe, M.D., Ph.D., Division of Nuclear Medicine and Molecular Imaging, The Russell H. Morgan Department of Radiology and Radiological Science, Johns Hopkins University School of Medicine, 601 N. Caroline St., Baltimore, MD 21287, Phone: (410) 502-1520, srowe8@jhmi.edu.

Conflict of Interest
Martin G. Pomper is a coinventor on a patent covering [^{18}F]DCFPyL and is entitled to a portion of any licensing fees and royalties generated by this technology. This arrangement has been reviewed and approved by the Johns Hopkins University in accordance with its conflict-of-interest policies. He has also received research funding from Progenics Pharmaceuticals, the licensee of [^{18}F]DCFPyL. Michael A. Gorin has served as a consultant to, and has received research funding from, Progenics Pharmaceuticals. Kenneth J. Pienta has received research funding from Progenics Pharmaceuticals. Steven P. Rowe has received research funding from Progenics Pharmaceuticals.

Purpose: In this study, we aimed to quantitatively investigate the biodistribution of [^{18}F]DCFPyL in patients with prostate cancer (PCa) and to determine whether uptake in normal organs correlates with an increase in tumor burden.

Procedures: 50 patients who had been imaged with [^{18}F]DCFPyL positron emission tomography/computed tomography (PET/CT) were retrospectively included in this study. 40/50 (80%) demonstrated radiotracer uptake on [^{18}F]DCFPyL PET/CT compatible with sites of PCa. Volumes of Interests (VOI) were set on normal organs (lacrimal glands, parotid glands, submandibular glands, liver, spleen, and kidneys) and on tumor lesions. Mean standardized uptake values corrected to lean body mass (SUL_{mean}) and mean standardized uptake values corrected to body weight (SUV_{mean}) for normal organs were assessed. For the entire tumor burden, $SUL_{mean/max}$, SUV_{mean}, tumor volume (TV), and the total activity in the VOI were obtained using tumor segmentation. A Spearman's rank correlation coefficient was used to investigate correlations between normal organ uptake and tumor burden.

Results: There was no significant correlation between TV with the vast majority of the investigated organs (lacrimal glands, parotid glands, submandibular glands, spleen, and liver). Only the kidney showed significant correlation: With an isocontour threshold at 50%, left kidney uptake parameters correlated significantly with TV (SUV_{mean}, $\rho = -0.214$ and SUL_{mean}, $\rho = -0.176$, $p < 0.05$, respectively).

Conclusions: Only a minimal sink effect with high tumor burden in patients imaged with [^{18}F]DCFPyL was observed. Other factors, such as a high intra-patient variability of normal organ uptake, may be a much more important consideration for personalized dosimetry with PSMA-targeted therapeutic agents structurally related to [^{18}F]DCFPyL than the tumor burden.

Keywords

Prostate-specific membrane antigen; positron emission tomography; biodistribution; [^{18}F]DCFPyL; PSMA

Introduction

Novel imaging agents targeting prostate-specific membrane antigen (PSMA) have demonstrated excellent diagnostic accuracy for visualizing sites of prostate cancer (PCa) [1–3]. Although Ga-68-labeled radiotracers targeting PSMA have been more commonly used, novel F-18 labeled radiotracers, such as [^{18}F]DCFPyL, are increasingly utilized and there have been suggestions of superior imaging characteristics relative to Ga-68 labeled compounds [4–7]. In a similar vein to the theranostics twins [^{68}Ga]/[^{177}Lu] 1,4,7,10-tetraazacyclododecane-N,N′,N″,N‴-tetraacetic acid-d-Phe(1)-Tyr(3)-octreotide/-octreotate(DOTATOC/-TATE) used for the diagnosis and treatment of neuroendocrine tumors (NET), the theranostic concept has been extended to PCa with the introduction of Lu-177-labeled PSMA-targeted compounds [8]. As a result, it is imperative to understand the fundamental factors that can affect PSMA-targeted radiotracer biodistribution and how those factors might affect both diagnostic accuracy and therapy planning. Indeed, the biodistribution of PSMA-targeted positron emission tomography (PET) imaging involves complex interplay of varying factors, such as renal excretion, physiologic uptake and retention in normal organs, normal variant uptake in benign lesions, and uptake in PCa tumor lesions.

As reported previously, radiotracers may be prone to the impact of tumor uptake on normal organ biodistribution [9–11]. For example, Beauregard, et al. reported declines in [^{68}Ga]DOTATATE uptake in normal organs in patients with increasing NET burden and suggested to adapt the therapeutic activity with a Lu-177 labeled compound to the tumor load [11]. In contrast, our group recently reported that there was no such tumor sink effect using the lower affinity somatostatin receptor imaging probe [^{68}Ga]DOTATOC [12]. In regards to PSMA-targeted radiotracers in patients with PCa, Gärtner, et al. reported on a decline of [^{68}Ga]PSMA-11 uptake in kidneys in patients with higher tumor burden [13].

Given the current trend towards increased use of F-18-labeled PSMA-ligands [4–5], we sought to investigate factors that may have an impact on semiquantitative parameters in PSMA-targeted PET Imaging with ^{18}F-DCFPyL: First, in a companion study, we aimed to investigate the inter-patient and intra-patient variability of semiquantitative parameters in the most relevant normal organs [14], while in the present paper, the biodistribution of [^{18}F]DCFPyL in PCa patients with different tumor burdens was quantitatively investigated. As this may have implications for a theranostic approach using Lu-177 labeled ligands structurally related to [^{18}F]DCFPyL, we aimed to clarify whether uptake in normal organs may correlate with an increase in tumor burden.

Methods

Patient Population.

In total, 50 patients with histologically proven PCa who had undergone [^{18}F]DCFPyL PET/computed tomography (CT) imaging were included in this evaluation. All patients were originally imaged as part of an institutional review board-approved protocol (Clinicaltrials.gov identifier NCT02825875) and signed written informed consent prior to imaging. The current study is a *post hoc* analysis of the referenced prospective trial. [^{18}F]DCFPyL was used under an Investigational New Drug application from the United States Food and Drug Administration (IND 121064). A detailed description of this patient cohort can be found in Table 1 [15].

Imaging Procedure

As per standard practice at our institution, patients were asked to be *nil per os* (with the exception of water and medications) for a minimum of 4 h prior to radiotracer injection. [^{18}F]DCFPyL was synthesized under current good manufacturing practice conditions as has been previously described [16]. Integrated PET/CT using either a Discovery RX 64-slice PET/CT (General Electric, Waukesha, Wisconsin, USA) or a Biograph mCT 128-slice PET/CT (Siemens, Erlangen, Germany) was performed in all patients. The PET scanners were operated in 3D emission mode with CT attenuation correction. [^{18}F]DCFPyL ≤333 MBq (≤9 mCi) was administered through a peripheral intravenous catheter and after an uptake time of approximately 60 min, acquisitions from the mid-thigh to the vertex of the skull were conducted, covering six to eight bed positions. The patients were in the supine position. For further details, please refer to [17].

Imaging Analysis

PET images were analyzed using XD3 Software (Mirada Medical, Oxford, UK). PET, CT, and hybrid PET/CT imaging overlays were assessed in the axial, sagittal, and coronal planes in all 50 patients. Lesions were identified as abnormal foci of radiotracer uptake above background and in expected patterns for PCa spread [18–19]. Lesions were selected by a single reader experienced in the interpretation of PSMA-targeted PET (MSJ) and verified by a second experienced reader (SPR).

The normal biodistribution of [^{18}F]DCFPyL, includes uptake in the lacrimal glands, parotid glands, and submandibular glands, as well as in the liver, spleen, kidneys, and bowel (predominantly proximal small bowel) [18–19]. For the lacrimal glands, major salivary glands, liver, spleen, and kidneys, volume of interests (VOIs) were manually set covering the entire organ volume using the best visual approximation of the organ edge on the PET images using previously described methodology [20]. Moreover, as described in [12], the entire volume of all [^{18}F]DCFPyL-avid tumor lesions (i.e., tumor burden) was manually segmented using the same procedure. The CT images were not used as a primary guide for the segmentation of the VOIs but were available as a reference to improve VOI placement in regions of complex anatomy or high background radiotracer uptake, as necessary [20].

For normal organs, the following parameters were recorded: mean standardized uptake value corrected to lean body mass (SUL_{mean}) and mean standardized uptake value corrected to body weight (SUV_{mean}) [17, 20]. For the entire tumor burden, the following parameters were assessed: SUL_{mean}, the maximum standardized uptake value corrected to lean body mass (SUL_{max}), SUV_{mean}, tumor volume (TV) and the fractional tumor activity (FTA) in the VOI. The latter parameter is well-established in the literature and has also been referred to as tumor lesion (TL)-PSMA [21–22]. FTA was calculated as follows: [TV x SUV_{mean}]. An isocontour threshold of 50% of the SUV_{max} were determined between the background and the maximal pixel value of the VOI.

Statistical Analysis

Percentiles are reported to describe the distribution of the parameters. Additionally, mean ± standard deviation are provided for parameters with a normal distribution as determined with the Shapiro-Wilk test. Spearman’s rank correlation coefficient (Spearman’s Rho, ρ) was used to assess the correlations between parameters. Statistical analysis was performed using MedCalc Statistical Software (version 18.2.1, MedCalc Software bvba, Ostend, Belgium). The statistical significance level was set at $p < 0.05$.

Results

Patient Population

The median age of the cohort was 65 ± 8 years (range, 44 – 77 years). The majority of the subjects were of white race (38/50, 76.0%). The clinical indications for performing an

[^{18}F]DCFPyL PET/CT were as follows: staging in 24/50 (48.0%), biochemical recurrence in 9/50 (18.0%), biochemical persistence after surgery in 6/50 (12.0%), primary diagnostic assessment in 5/50 (10.0%), potential withdrawal of hormonal therapy in 3/50 (6.0%), and other reasons in 3/50 (6.0%). The median prostate specific antigen level was 3.2 ng/ml (0.02 — 48) and 41/50 (82.0%) patients had therapy prior to [^{18}F]DCFPyL PET/CT: surgery in 29/41 (70.7%), hormonal therapy in 21/41 (51.2%), radiotherapy in 18/41 (43.9%) and chemotherapy in 6/41 (14.6%). Additional details of the study population are provided in Table 1.

Quantitative Assessment

In those patients with discernible tumor radiotracer uptake (n = 40), a total of 243 VOIs were placed (median, 3 per patient; range, 1 - 78) to generate data for tumor burden. 137/243 (56.4%) of the VOIs were set on bone lesions, 87/243 (35.8%) were placed on lymph nodes (LNs), 13/243 (5.3%) were placed on non-LN soft tissue sites, 5/243 (2.1%) were placed on lung lesions and one (0.4%) VOI was placed on a liver lesion. For normal organs, the following values (median) were recorded: For SUL_{mean}: left lacrimal gland 3.6 and right lacrimal gland 3.7; left parotid gland 6.0 and right parotid gland 6.3; left submandibular gland 5.8 and right submandibular gland 5.9; liver 3.7; spleen 2.6; left kidney 16.6 and right kidney 17.3. For SUV_{mean}: left lacrimal gland 4.9 and right lacrimal gland 5.1; left parotid gland 8.1 and right parotid gland 8.2; left submandibular gland 7.9 and right submandibular gland 8.0; liver 5.0; spleen 3.7; left kidney 22.8 and right kidney 23.4. For tumor burden, the median values for SUL_{mean}, SUL_{max}, SUY_{mean}, TV, and FTAare displayed in Table 2.

Correlative Analysis between tumor burden vs. normal organ uptake and inter-organ correlations

There was no significant correlation between TV with the vast majority of the investigated organs (lacrimal glands, parotid glands, submandibular glands, spleen and liver). Only the kidney showed significant correlations with tumor burden parameters: SUV_{mean} and SUL_{mean} of the left kidney correlated with TV using an intensity threshold of 50% (Table 3: SUV_{mean}, $\rho = -0.214$ and SUL_{mean}, $p = -0.176$, $p < 0.05$, respectively, Fig. 1a and b). Table 3 displays Spearman’s Rho and Fig. 1 demonstrates correlative plots for the relations between normal organs and tumor burden. Figure 2 displays three patients with different tumor burden: **a** low, **b** intermediate, and **c** high and reflects visually no significant decrease in normal organ uptake with increasing tumor burden.

Discussion

PSMA-targeted radiotracers such as [^{18}F]DCFPyL have demonstrated significantly improved imaging characteristics for identifying sites of PCa relative to conventional imaging [6, 23]. The widespread use of these agents and their ability to select patients for PSMA-targeted therapies necessitates a complete understanding of the parameters that dictate normal organ uptake. As such, in this manuscript we aimed to continue an exploration of the factors that may influence semiquantification of [^{18}F]DCFPyL studies. Thus, in a companion paper, the impact of intra-/inter-patient variability on relevant normal organs was assessed [14], while in the present study, we investigated the impact of tumor burden on normal organ uptake.

First and foremost, the majority of the herein investigated organs (lacrimal glands, parotid glands, submandibular glands, spleen, and liver) did not show significant correlations with any of the parameters assessing the tumor burden. Only a moderate significant inverse correlation for the kidneys with TV was on the left side (Fig. 1a and b). Such findings have also been observed with a Ga-68-labeled PSMA agent using an isocontour threshold of 50% [13]. Notably, the correlation coefficients were rather low in the previous investigation, and this was similar to the herein obtained ρ values [13]. Nonetheless, in the present study, the sink effect was not observed across all of the studied organs. Thus, given the minimal impact of uptake on normal organs in patients with higher tumor burden, other factors may play a more crucial role in dosimetry with [^{18}F]DCFPyL. In a further analysis of our research group investigating the inter-patient and intra-patient variability of semiquantitative parameters in the most relevant normal organs, significant variability in [^{18}F]DCFPyL uptake was noted [14]: over time, the liver and kidneys showed the greatest degree of variability for intrapatient factors (e.g. time of day, recent meals, hydration status, and therapies during the time interval between subsequent [^{18}F]DCFPyL scans). This was in contradistinction to the variability in normal lacrimal glands, salivary glands, and spleen, which primarily depend upon inter-patient factors (e.g. weight, height, body composition, and differences in prior therapies) [14]. Thus, integrating the available information of our two studies investigating semiquantitative parameters with [^{18}F]DCFPyL, the inter-/intra-patient variability would be a much more important consideration for personalized dosimetry with PSMA-targeted therapeutic agents structurally related to [^{18}F]DCFPyL than the tumor burden.

In light of the present study showing no tumor sink effect with [^{18}F]DCFPyL, a peritherapeutic dosimetry for RLT planning may serve as an attractive alternative for a more reliable dose estimate. Albeit such a procedure may be challenging for both patients and personnel [24–25], it may be considered for every individual to safely determine the appropriate amount of activity to be administered in a therapeutic setting [26]. Extrapolation of the results of this study to therapeutic radionuclides that are structurally similar to [^{18}F]DCFPyL but still vary in aspects of their chemical structures must be made with caution, although the similar biodistributions of many PSMA-targeted agents suggests that these findings may still be directly relevant.

The present study has several limitations: First, a larger assessment with more patients is warranted to confirm our preliminary findings. However, on an intra-tumor parameter level, highly significant correlations were achieved, which may serve as quality control metrics for the present study (data not shown). Apart from that, one may speculate if a more sustainable tumor sink effect (e.g. in the kidneys) may be achieved if more patients with higher tumor burden are included [13]. However, the current *post hoc* analysis also investigated such superscans (e.g. with extensive skeletal involvement, Fig. 2c) and the randomly selected cases may rather reflect a more “real-world” scenario, as no preselection of patients with different amounts of tumor burden was conducted. Nonetheless, the herein derived results even in patients with rather low tumor burden may be of utmost importance, as PSMA-PET is more routinely used in patients with low or even ultra-low PSA levels [27].

Conclusion

In the present analysis with the PSMA-targeted radiotracer [^{18}F]DCFPyL, only a modest tumor sink effect was observed for selected uptake parameters for the kidneys whereas for most normal organs, no sink effect was seen. While statistically significant, the effect in the kidneys is very small (ρ, range, −0.176 to −0.214) and unlikely to be clinically relevant. Thus, other factors, such as the relatively high intra-patient variability for normal organ uptake described in our companion paper, may be a much more important considerations for personalized dosimetry with PSMA-targeted therapeutic agents structurally related to [^{18}F]DCFPyL.

Acknowledgments

Sources of Funding

Progenics Pharmaceuticals, The Prostate Cancer Foundation Young Investigator Award, and National Institutes of Health grants CA134675, CA183031, CA184228, and EB024495.

REFERENCES

1. Gorin MA, Pomper MG, Rowe SP (2016) PSMA-targeted imaging of prostate cancer: the best is yet to come. BJU Int 117:715–716. [PubMed: 27079480]
2. Sheikhbahaei S, Afshar-Oromieh A, Eiber M, et al. (2017) Pearls and pitfalls in clinical interpretation of prostate-specific membrane antigen (PSMA)-targeted PET imaging. Eur J Nucl Med Mol Imaging 44:2117–2136. [PubMed: 28765998]
3. Eiber M, Herrmann K, Fendler WP, Maurer T (2016) ^{68}Ga-labeled Prostate-specific Membrane Antigen Positron Emission Tomography for Prostate Cancer Imaging: The New Kid on the Block-Early or Too Early to Draw Conclusions? Eur Urol 70:938–940. [PubMed: 27481174]
4. Kesch C, Kratochwil C, Mier W, et al. (2017) ^{68}Ga or ^{18}F for Prostate Cancer Imaging? J Nucl Med 58:687–688. [PubMed: 28408526]
5. Szabo Z, Mena E, Rowe SP, et al. (2015) Initial Evaluation of [^{18}F]DCFPyL for Prostate-Specific Membrane Antigen (PSMA)-Targeted PET Imaging of Prostate Cancer. Mol Imaging Biol 17:565–574. [PubMed: 25896814]
6. Dietlein M, Kobe C, Kuhnert G, et al. (2015) Comparison of [^{18}F]DCFPyL and [^{68}Ga]Ga-PSMA-HBED-CC for PSMA-PET Imaging in Patients with Relapsed Prostate Cancer. Mol Imaging Biol 17:575–584. [PubMed: 26013479]
7. Werner RA, Andree C, Javadi MS, et al. (2018) A Voice From the Past: Rediscovering the Virchow Node With Prostate-specific Membrane Antigen-targeted ^{18}F-DCFPyL Positron Emission Tomography Imaging. Urology 117:18–21. [PubMed: 29626569]
8. Werner RA, Weich A, Kircher M, et al. (2018) The theranostic promise for Neuroendocrine Tumors in the late 2010s - Where do we stand, where do we go? Theranostics 8:6088–6100. [PubMed: 30613284]
9. Prasad V, Baum RP (2010) Biodistribution of the Ga-68 labeled somatostatin analogue DOTA-NOC in patients with neuroendocrine tumors: characterization of uptake in normal organs and tumor lesions. Q J Nucl Med Mol Imaging 54:61–67. [PubMed: 20168287]
10. Liu Y (2011) Super-superscan on a bone scintigraphy. Clin Nucl Med 36:227–228. [PubMed: 21285685]

11. Beauregard JM, Hofman MS, Kong G, Hicks RJ (2012) The tumour sink effect on the biodistribution of ^{68}Ga-DOTA-octreotate: implications for peptide receptor radionuclide therapy. Eur J Nucl Med Mol Imaging 39:50–56. [PubMed: 21932117]
12. Werner RA, Hanscheid H, Leal JP, et al. (2018) Impact of Tumor Burden on Quantitative [^{68}Ga] DOTATOC Biodistribution. Mol Imaging Biol.
13. Gaertner FC, Halabi K, Ahmadzadehfar H, et al. (2017) Uptake of PSMA-ligands in normal tissues is dependent on tumor load in patients with prostate cancer. Oncotarget 8:55094–55103. [PubMed: 28903405]
14. Sahakyan K, Li X, Lodge MA, et al. (2018) Semiquantitative Parameters in PSMA-Targeted PET Imaging with ^{18}F-DCFPyL: Intrapatient and Interpatient Variability of Normal Organ Uptake
15. Werner RA, Bundschuh RA, Bundschuh L, et al. (2018) Interobserver Agreement for the Standardized Reporting System PSMA-RADS 1.0 on ^{18}F-DCFPyL PET/CT Imaging. J Nucl Med.
16. Ravert HT, Holt DP, Chen Y, et al. (2016) An improved synthesis of the radiolabeled prostate-specific membrane antigen inhibitor, [^{18}F]DCFPyL. J Labelled Comp Radiopharm 59:439–450. [PubMed: 27470935]
17. Werner RA, Sheikhbahaei S, Jones KM, et al. (2017) Patterns of uptake of prostate-specific membrane antigen (PSMA)-targeted ^{18}F-DCFPyL in peripheral ganglia. Ann Nucl Med 31:696–702. [PubMed: 28831739]
18. Rowe SP, Pienta KJ, Pomper MG, Gorin MA (2018) PSMA-RADS Version 1.0: A Step Towards Standardizing the Interpretation and Reporting of PSMA-targeted PET Imaging Studies. Eur Urol 73:485–487. [PubMed: 29132714]
19. Rowe SP, Pienta KJ, Pomper MG, Gorin MA (2018) Proposal for a Structured Reporting System for Prostate-Specific Membrane Antigen-Targeted PET Imaging: PSMA-RADS Version 1.0. J Nucl Med 59:479–485. [PubMed: 28887401]
20. Li X, Rowe SP, Leal JP, et al. (2017) Semiquantitative Parameters in PSMA-Targeted PET Imaging with (18)F-DCFPyL: Variability in Normal-Organ Uptake. J Nucl Med 58:942–946. [PubMed: 27932557]
21. Schmidkonz C, Cordes M, Schmidt D, et al. (2018) ^{68}Ga-PSMA-11 PET/CT-derived metabolic parameters for determination of whole-body tumor burden and treatment response in prostate cancer. Eur J Nucl Med Mol Imaging 45:1862–1872. [PubMed: 29725716]
22. Schmuck S, von Klot CA, Henkenberens C, et al. (2017) Initial Experience with Volumetric ^{68}Ga-PSMA I&T PET/CT for Assessment of Whole-Body Tumor Burden as a Quantitative Imaging Biomarker in Patients with Prostate Cancer. J Nucl Med 58:1962–1968. [PubMed: 28522740]
23. Rowe SP, Macura KJ, Mena E, et al. (2016) PSMA-Based [^{18}F]DCFPyL PET/CT Is Superior to Conventional Imaging for Lesion Detection in Patients with Metastatic Prostate Cancer. Mol Imaging Biol 18:411–419. [PubMed: 27080322]
24. Hanscheid H, Lapa C, Buck AK, Lassmann M, Werner RA (2018) Dose Mapping After Endoradiotherapy with ^{177}Lu-DOTATATE/DOTATOC by a Single Measurement After 4 Days. J Nucl Med 59:75–81. [PubMed: 28588150]
25. Hanscheid H, Lapa C, Buck AK, Lassmann M, Werner RA (2017) Absorbed dose estimates from a single measurement one to three days after the administration of ^{177}Lu-DOTATATE/-TOC. Nuklearmedizin 56:219–224. [PubMed: 29533417]
26. Eberlein U, Cremonesi M, Lassmann M (2017) Individualized Dosimetry for Theranostics: Necessary, Nice to Have, or Counterproductive? J Nucl Med 58:97S–103S. [PubMed: 28864620]
27. Giesel FL, Knorr K, Spohn F, et al. (2019) Detection Efficacy of ^{18}F-PSMA-1007 PET/CT in 251 Patients with Biochemical Recurrence of Prostate Cancer After Radical Prostatectomy. J Nucl Med 60:362–368. [PubMed: 30042163]

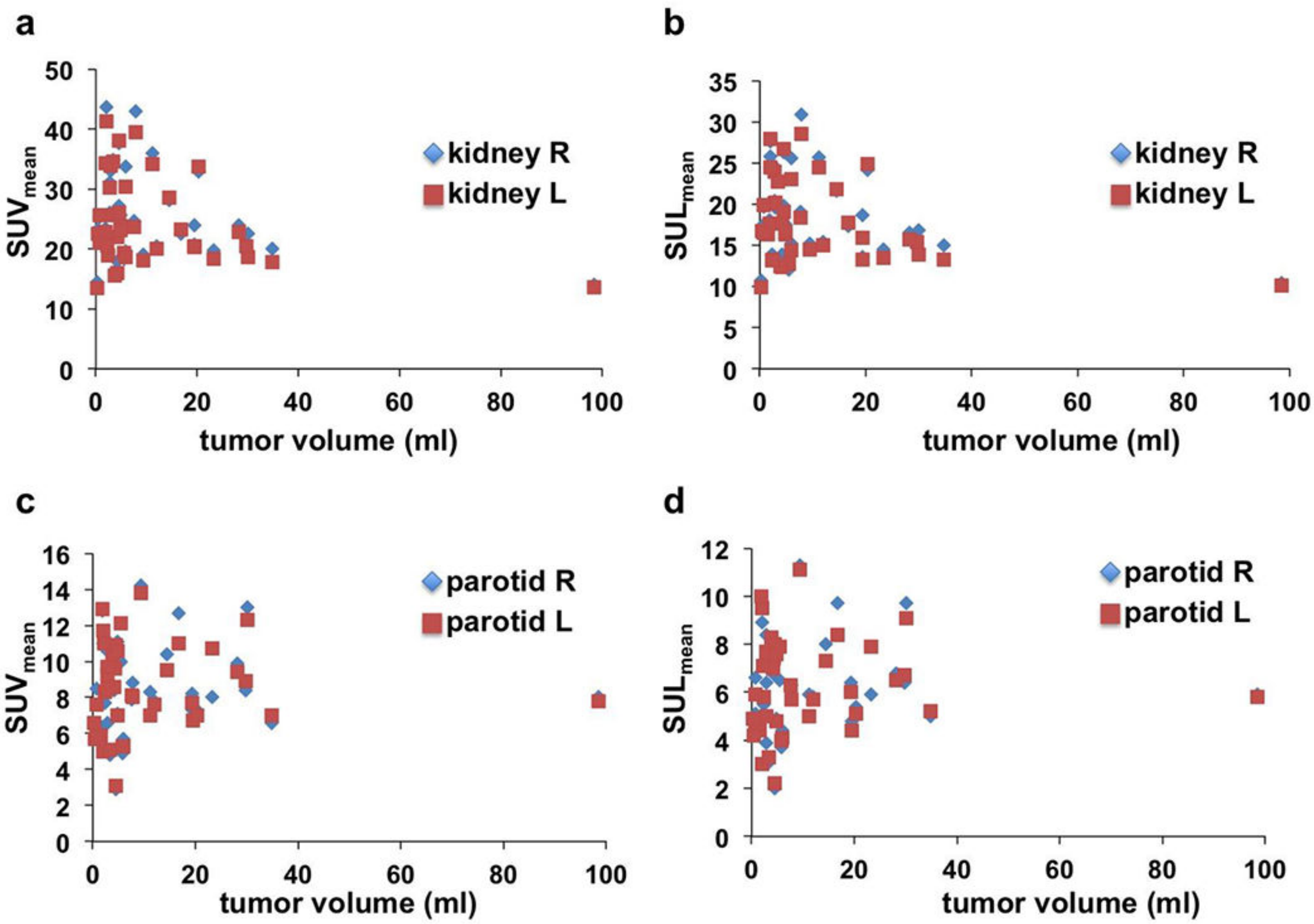
a
SUV_{mean}
50
40
30
20
10
0
0
20
40
60
80
100
tumor volume (ml)
◆kidney R
■kidney L
b
SUL_{mean}
35
30
25
20
15
10
5
0
0
20
40
60
80
100
tumor volume (ml)
◆kidney R
■kidney L
c
SUV_{mean}
16
14
12
10
8
6
4
2
0
0
20
40
60
80
100
tumor volume (ml)
◆parotid R
■parotid L
d
SUL_{mean}
12
10
8
6
4
2
0
0
20
40
60
80
100
tumor volume (ml)
◆parotid R
■parotid L

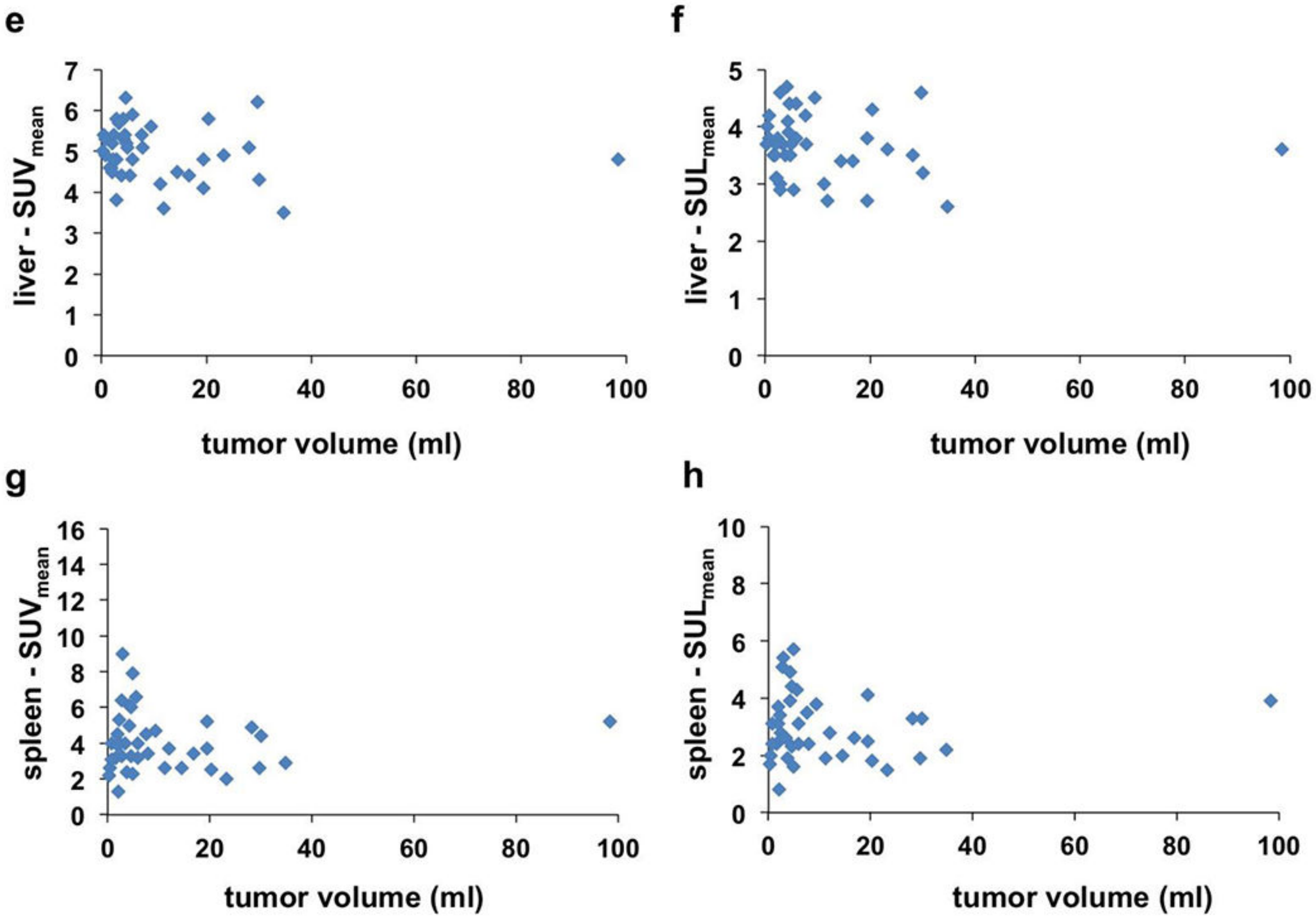

Figure 1.

Correlative plots of uptake in selected normal organs with [^{18}F]DCFPyL derived tumor volume (intensity threshold, 50%). The **a** SUV$_{mean}$ and **b** SUL$_{mean}$ of the left kidney (red) correlated significantly with tumor volume ($p < 0.05$). **a** SUV$_{mean}$ and b SUL$_{mean}$ of the left (L) and right (R) kidneys, **c** SUV$_{mean}$ and **d** SUL$_{mean}$ of the left and right parotid glands, **e** SUV$_{mean}$ and **f** SUL$_{mean}$ of the liver, **g** SUV$_{mean}$ and **h** SUL$_{mean}$ of the spleen. SUV$_{mean}$ = mean standardized uptake value corrected to body weight, SUL$_{max}$ = the maximum standardized uptake value corrected to lean body mass.

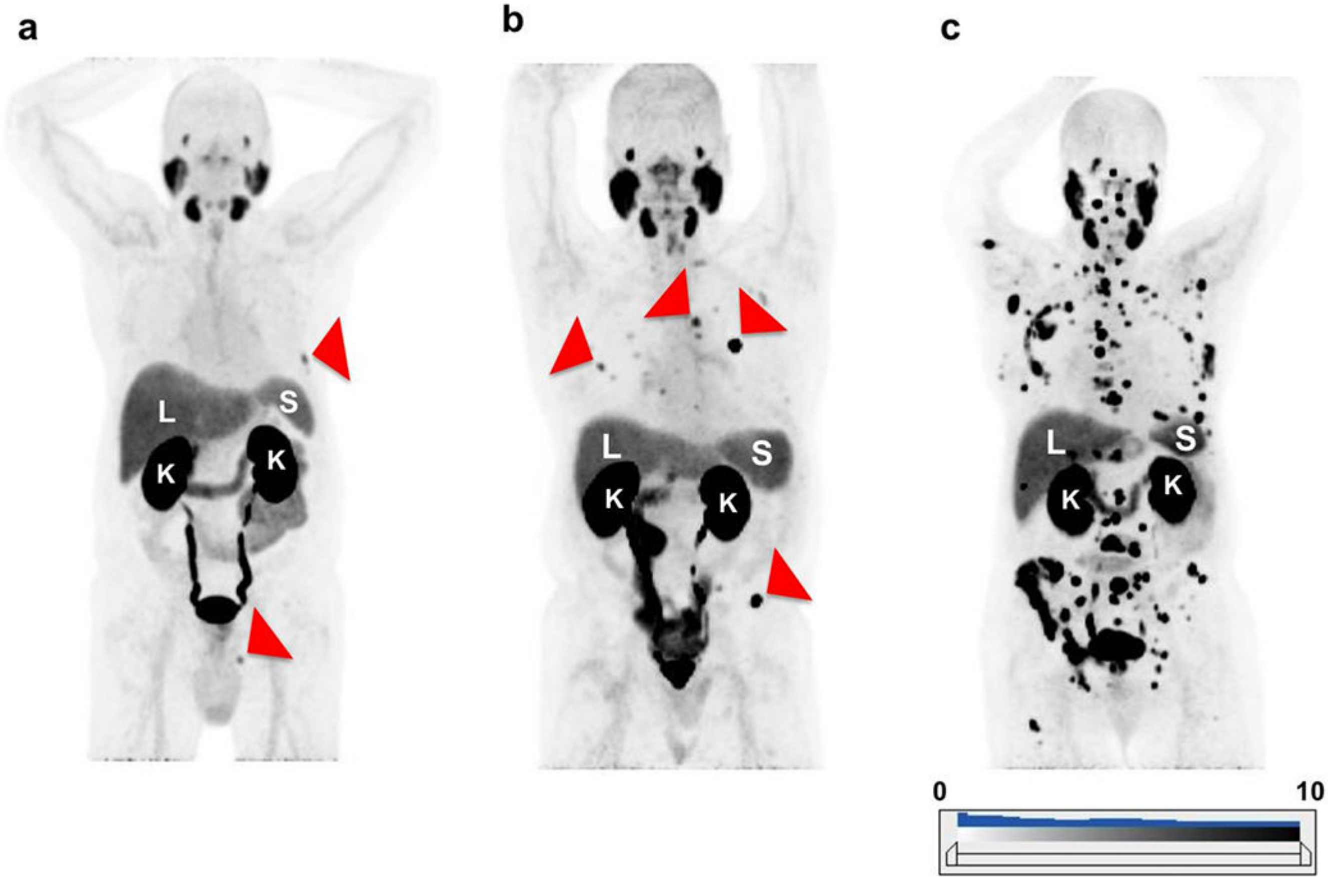

Figure 2.

[^{18}F]DCFPyL maximum intensity projection (MIP) of patients with **a** low, **b** intermediate and **c** high tumor burden. Spleen (S), liver (L) and kidneys (K) are indicated. Red arrows indicate representative tumor lesions, which can be detected on the MIPs: In Patient **a**: metatases in the 7th rib (left) and in the left ischium are indicated. In Patient **b**: multiple bone lesions are indicated. Patient **c** shows a near-superscan with extensive involvement in the skeleton. The uptake in normal organs (visible for liver, kidneys, and spleen) does not differ visually among the different patients.

Table 1.

Detailed patients' characteristics.

Age (median ± SD, in years)		**65 ± 8**
Height (m)		1.78 ± 0.06
Weight (kg)		88 ± 15
Indication for Scan	Staging	24/50 (48%)
	Biochemical Reccurence	9/50 (18%)
	Biochemical Persistence after Primary Surgery	6/50 (12%)
	Primary Diagnosis	5/50 (10%)
	Potential withdrawal of androgen deprivation therapy	3/50 (6%)
	Other	3/50 (6%)
PSA level (ng/ml)	Overall (median (range))	3.2 (0.02 – 48)
Prior therapies	in total	41/50 (82%)
	Surgery	29/41 (70.7%)
	Hormonal Therapy	21/41 (51.2%)
	RTx	18/41 (43.9%)
	CTx	6/41 (14.6%)

SD = standard deviation, CTx = chemotherapy, PSA = prostate specific antigen, RTx = radiation therapy. Modified from *Werner* et al. [14], © by the Society of Nuclear Medicine and Molecular Imaging.

Table 2.

Descriptive statistics of normal organs and tumor burden.

Compartment	Parameter	Minimum	Median	Maximum	Mean[*]	StDev[*]
Lacrimal Gland L	**SUL**$_{mean}$	1.8	3.6	5.2	3.7	0.7
	SUV$_{mean}$	2.4	4.9	6.7	5	0.9
Lacrimal Gland R	**SUL**$_{mean}$	2.4	3.7	5.6	3.7	0.7
	SUV$_{mean}$	3.3	5.1	7	5.1	0.9
Parotid Gland L	**SUL**$_{mean}$	3	6	11.1	6.2	1.9
	SUV$_{mean}$	5	8.1	13.8	8.3	2.4
Parotid Gland R	**SUL**$_{mean}$	2	6.3	11.3	6.3	1.9
	SUV$_{mean}$	4.9	8.2	14.2	8.5	2.4
SMG L	**SUL**$_{mean}$	3.3	5.8	13.5		
	SUV$_{mean}$	5	7.9	17.5		
SMG R	**SUL**$_{mean}$	1.9	5.9	13.1		
	SUV$_{mean}$	4	8	16.8		
Liver	**SUL**$_{mean}$	2.6	3.7	4.7	3.7	0.5
	SUV$_{mean}$	3.5	5	6.3	5	0.7
Spleen	**SUL**$_{mean}$	0.8	2.6	7.8		
	SUV$_{mean}$	1.3	3.7	14.4		
Kidney L	**SUL**$_{mean}$	7.8	16.6	28.7	17.4	5
	SUV$_{mean}$	10.5	22.8	41.3		
Kidney R	**SUL**$_{mean}$	11.4	17.3	30.9	18.1	5
	SUV$_{mean}$	11.2	23.4	43.6		
Tumor Burden	**SUL**$_{mean}$	1.3	3.9	42.9		
	SUL$_{max}$	1.7	5.3	55.6		
	SUV$_{mean}$	1.6	5.4	57.9		
	TV	0.3	4.8	98.4		
	FTA	1.0	25.9	1752		

SUL$_{mean}$ = mean standardized uptake value corrected to lean body mass, SUV$_{mean}$ = mean standardized uptake value corrected to body weight, SMG = submandibular gland, SUL$_{max}$ = the maximum standardized uptake value corrected to lean body mass, TV = Tumor Volume (in ml), FTA = fractional tumor activity in the volume of interest.

[*] Mean and standard deviation (StDev) are not shown when the Shapiro-Wilk test excluded a normal distribution. L = center, R = right.

Table 3.

Correlation between organ-derived values and tumor burden based on [^{18}F]DCFPyL PET. Spearman's Rho (ρ), and the 2-sided significance P is shown. The following tumor burden parameters are displayed: SUV_{mean} = mean standardized uptake value corrected to body weight, $SUL_{mean/max}$ = mean/maximum standardized uptake value corrected to lean body mass, TV = Tumor Volume, FTA = fractional tumor activity in the volume of interest. Submandibular glands (SMG). Significant parameters are marked in bold. * $p < 0.05$.

			Tumor Burden-derived parameters				
			SUV_{mean}	**SUL_{mean}**	**SUL_{max}**	**TV**	**FTA**
Kidney L	SUV_{mean}	ρ	−0.152	−0.161	−0.22	−0.214	−0.226
		P	0.54	0.46	0.41	0.049*	0.160
	SUL_{mean}	ρ	−0.232	−0.24	−0.282	−0.176	−0.255
		P	0.14	0.12	0.09	0.041*	0.112
Kidney R	SUV_{mean}	ρ	−0.147	−0.167	−0.204	−0.137	−0.160
		P	0.64	0.3	0.52	0.06	0.325
	SUL_{mean}	ρ	−0.23	−0.25	−0.28	−0.165	−0.245
		P	0.18	0.14	0.12	0.05	0.127
Parotid L	SUV_{mean}	ρ	−0.129	−0.088	−0.081	0.148	0.012
		P	0.39	0.55	0.67	0.79	0.944
	SUL_{mean}	ρ	−0.154	−0.117	−0.103	0.148	−0.002
		P	0.26	0.37	0.45	0.4	0.992
Parotid R	SUV_{mean}	ρ	−0.188	−0.155	−0.168	0.167	−0.010
		P	0.29	0.37	0.37	0.71	0.952
	SUL_{mean}	ρ	−0.188	−0.155	−0.168	0.125	−0.046
		P	0.2	0.36	0.26	0.4	0.779
Lacrimal Gland L	SUV_{mean}	ρ	−0.038	−0.008	−0.012	0.041	0.037
		P	0.81	0.96	0.94	0.8	0.823
	SUL_{mean}	ρ	−0.099	−0.078	−0.064	0.069	−0.018
		P	0.54	0.63	0.7	0.67	0.912
Lacrimal Gland R	SUV_{mean}	ρ	0.044	0.053	0.083	0.044	−0.005
		P	0.78	0.74	0.61	0.79	0.974
	SUL_{mean}	ρ	−0.037	0.003	−0.021	0.05	−0.061
		P	0.82	0.99	0.9	0.76	0.708
SMG L	SUV_{mean}	ρ	−0.311	−0.28	−0.263	0.292	0.014
		P	0.05	0.08	0.1	0.067	0.933
	SUL_{mean}	ρ	−0.269	−0.255	−0.237	0.246	−0.004
		P	0.09	0.11	0.14	0.13	0.982
SMG R	SUV_{mean}	ρ	−0.238	−0.213	−0.215	0.352	0.108
		P	0.14	0.19	0.18	0.03	0.509

			Tumor Burden-derived parameters				
			SUV_{mean}	**SUL_{mean}**	**SUL_{max}**	**TV**	**FTA**
	SUL_{mean}	ρ	−0.247	−0.232	−0.231	0.287	0.044
		P	0.12	0.15	0.15	0.07	0.789
Spleen	SUV_{mean}	ρ	−0.214	−0.171	−0.244	0.005	−0.199
		P	0.283	0.582	0.523	0.99	0.219
	SUL_{mean}	ρ	−0.23	0.18	−0.25	−0.028	−0.234
		P	0.14	0.31	0.26	0.96	0.146
Liver	SUV_{mean}	ρ	0.005	0.001	−0.037	−0.172	−0.136
		P	0.9	0.9	0.8	0.3	0.402
	SUL_{mean}	ρ	−0.119	−0.114	−0.154	−0.15	−0.243
		P	0.29	0.31	0.23	0.47	0.132